

Electronic Supplementary Information

Exploring the effect of nanocrystal facet orientations in g-C₃N₄/BiOCl heterostructures on photocatalytic performance

Qingbo Li^a, Xian Zhao^b, Jun Yang^c, Chun-Jiang Jia^a, Zhao Jin^a and Weiliu Fan^{a*}

^a Key Laboratory for Colloid and Interface Chemistry of State Educating Ministry, School of Chemistry and Chemical Engineering, Shandong University, Jinan 250100, China. Fax: +86-531-88364864; Tel: +86-531-88366330; E-mail: fwl@sdu.edu.cn

^b State Key Laboratory of Crystal Materials, Shandong University, Jinan 250100, China

^c State Key Laboratory of Multiphase Complex Systems, Institute of Process Engineering, Chinese Academy of Sciences, Beijing, 100190, China

Financial support from the National Natural Science Foundation of China (Grant no.: 21173131) and the Taishan Scholar Project of Shandong Province is gratefully acknowledged.

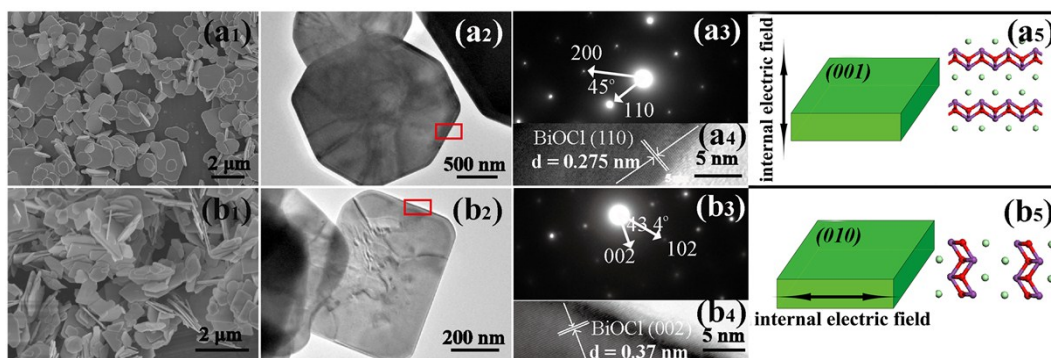


Fig. S1 Morphology and structure of BOC-001 and BOC-010 nanosheets: (a₁,b₁) SEM images, (a₂,b₂) TEM images, (a₃,b₃) SAED patterns, and (a₄,b₄) HRTEM images of pure BOC-001 and BOC-010. (a₅, b₅) Model showing the direction of the internal electric field and atomic structure (side view) of BOC-001 and BOC-010.

The as-synthesized BOC-001 and BOC-010 nanosheets present well-defined sheet-shaped structures with widths of 1-5 μm and 0.5-2 μm , respectively (Fig. S1a₁, a₂ and b₁, b₂). The SAED patterns demonstrate that the BiOCl nanosheets are well-crystallized single crystals. The corresponding SAED pattern of BOC-001 can be indexed as the [001] zone axis of tetragonal BiOCl, and the angle between the (110) and (200) planes is 45°, which is identical to the theoretical value (Fig. S1a₃). The interplanar spacing of 0.275 nm corresponds to the distance between (110) planes (Fig. S1a₄). Based on the above results, the bottom and top surfaces of the BOC-001 sample are identified as {001} facets. Fig. S1a₅ shows the atomic structure of BOC-001. [Bi₂O₂] slabs are interleaved by double slabs of Cl atoms along the [001] direction, therefore, the self-induced internal electric fields are perpendicular to the surfaces of BOC-001. For the BOC-010 sample, the corresponding SAED pattern can be indexed as the [010] zone, with an angle of 43.4°, which is identical to that between (102) and (002) faces (Fig. S1b₃). The lattice fringes of 0.37 nm correspond to the (002) atomic planes (Fig. S1b₄). It can be concluded that the main exposed interfaces of BOC-010 are {010} facets. The self-induced internal electric fields are parallel to the surfaces of BOC-010 (Fig. S1b₅).

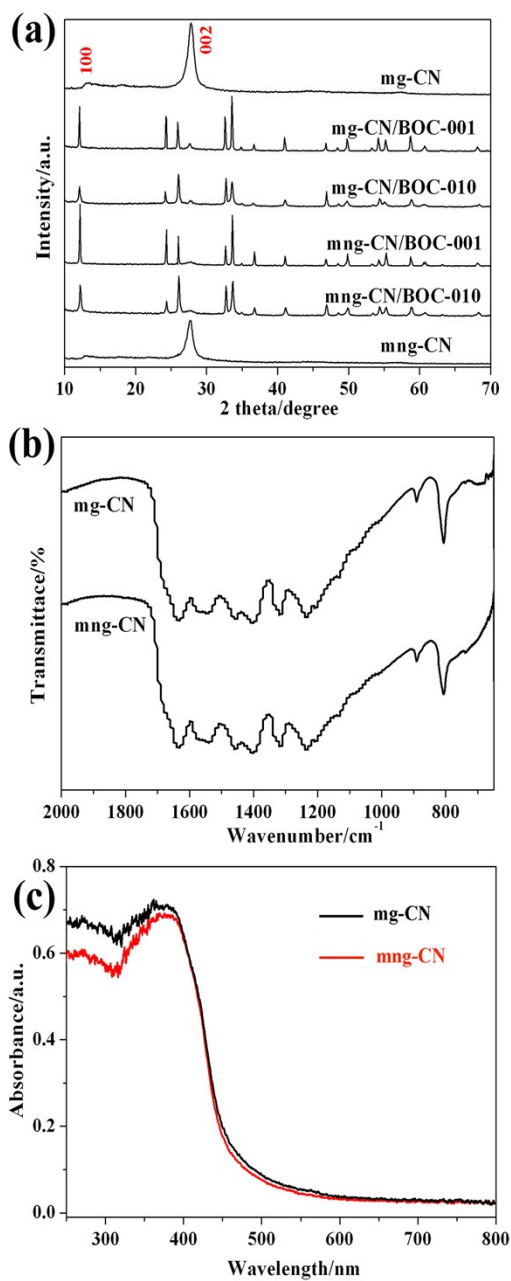


Fig. S2 (a) XRD patterns of mg-CN, mg-CN/BOC-001, mg-CN/BOC-010, mng-CN, mng-CN/BOC-001, and mng-CN/BOC-010. (b) FT-IR spectra of mg-CN and mng-CN. (c) UV-Vis spectra of mg-CN and mng-CN.

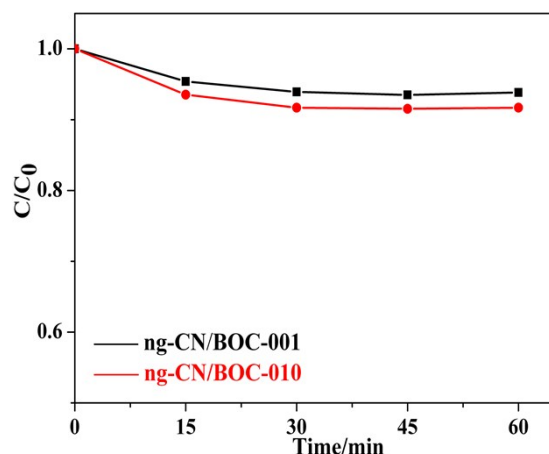


Fig. S3 Adsorption of MO over the ng-CN/BOC-001 and ng-CN/BOC-010 in the dark as a function of time.

In order to confirm the establishment of adsorption/desorption equilibrium between the photocatalyst and the degrading pollutants, the suspension was stirred in darkness for 1 h. The results show that the MO concentration remains unchanged after 30 min, indicating that the dark adsorption equilibrium was established within 30 min. The tiny difference of the adsorption ability between the two samples indicates that the adsorption process is not a critical factor in the degradation experiment in our work.

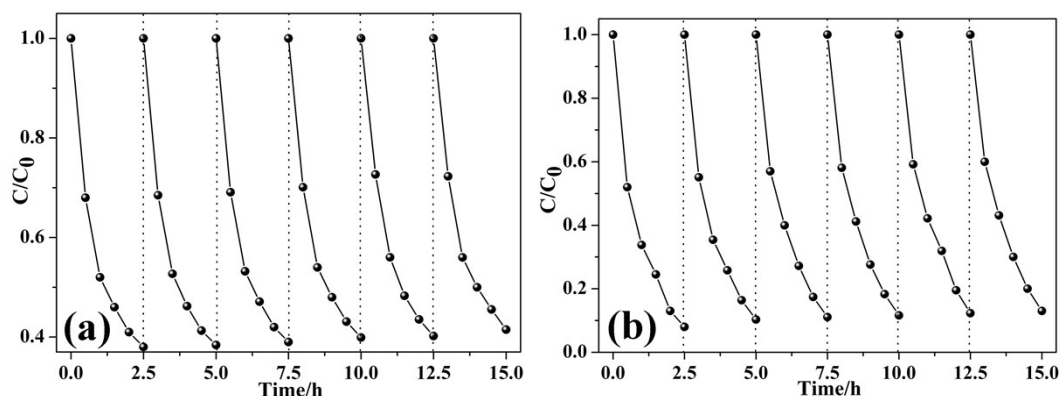


Fig. S4 Reusability of the ng-CN/BOC-001 (a) and ng-CN/BOC-010 (b) heterojunction photocatalysts in MO degradation.

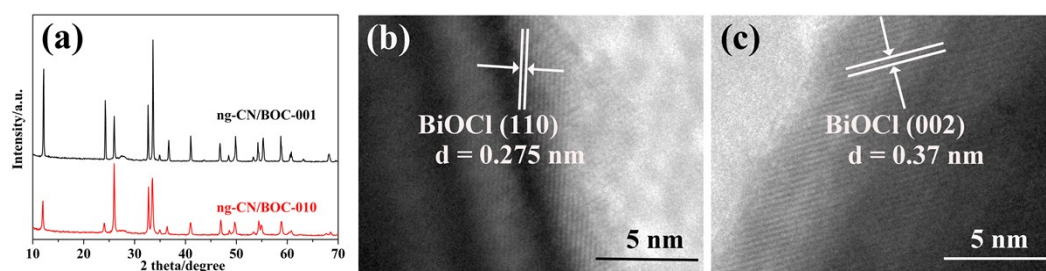


Fig. S5 (a) XRD patterns of the ng-CN/BiOCl after photocatalytic reaction. HRTEM images of (b) ng-CN/BOC-001 and (c) ng-CN/BOC-010 after photocatalytic reaction.

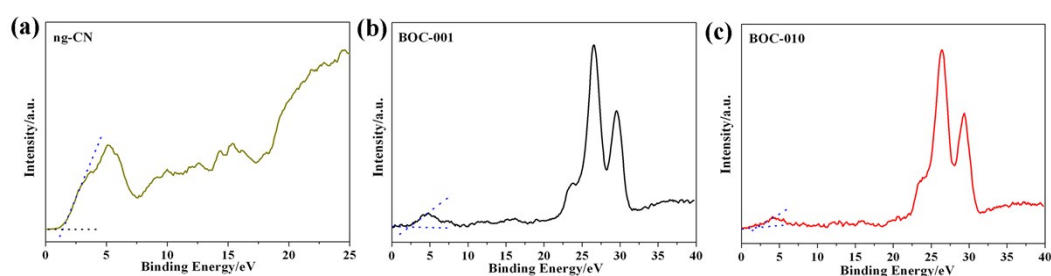


Fig. S6 VB XPS spectra of ng-CN (a), BOC-001 (b), and BOC-001 (c), respectively.

Table S1. Parameters of equivalent circuits for the impedance data of ng-CN, BiOCl-001, BiOCl-010, ng-CN/BiOCl-001, and ng-CN/BiOCl-001.

Samples	R_{ct} (10^5 , Ω)	R_s (10^5 , Ω)
ng-CN	1.55	29.36
BOC-001	2.41	44.34
BOC-010	10.37	65.31
ng-CN/BOC-001	1.03	26.43
ng-CN/BOC-010	0.60	10.12

Computational Details

First-principles calculations were carried out based on density functional theory (DFT) with the projector-augmented wave (PAW) method,¹ as implemented in the Vienna ab initio simulation package (VASP).² The kinetic energy cutoff for the plane wave basis set was chosen to be 400 eV. The k-meshes of 4×4×4 were adopted to sample

the first brillouin zone of the conventional unit cell. The standard DFT with generalized gradient approximation (GGA)³ functional of Perdew, Burke and Ernzerhof (PBE) was used to optimize the system geometry and the structure was fully relaxed until the maximum Hellmann-Feynman forces acting on each atom is less than 0.02 eV/Å. The electronic band structure was calculated by the hybrid functional (HSE06)^{4,5} methods based on the optimized structure.

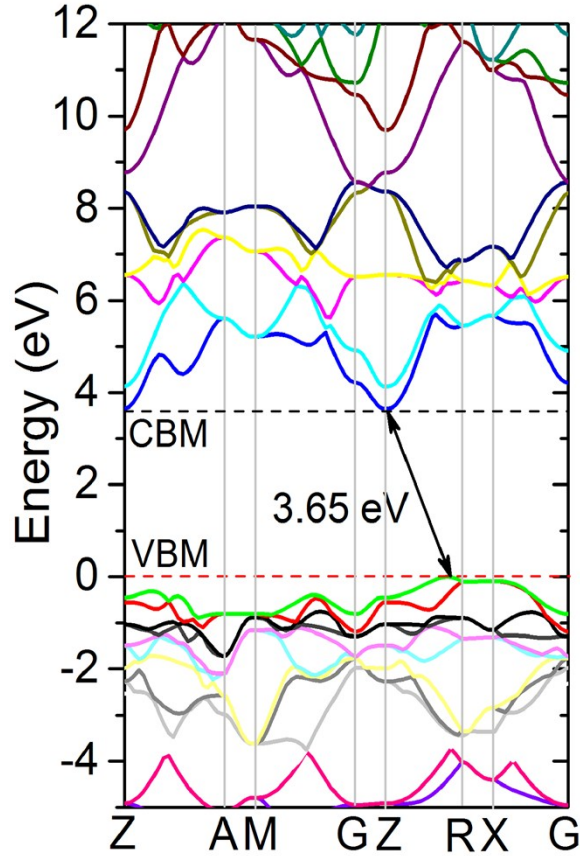


Fig. S7 Calculated electronic band structure of BiOCl.

The calculated electronic band structure of BiOCl is displayed in Fig. S6. According to our calculation, the band gap is 3.65 eV, which is in good accordance with the experimental result. The effective mass of photogenerated electron–holes can reflect the ability to transfer along special directions. The electronic effective mass (m_e^*) along various directions are calculated by fitting parabolic functions to CBM of BiOCl according to Equation 1:

$$\frac{1}{m_e^*} = \frac{1}{\hbar^2} \frac{\partial^2 E(\kappa)}{\partial \kappa^2}. \quad 1$$

Here, \hbar is rationalized Planck constant, and k is the vector of reciprocal space. Based on the calculated results, the electron effective mass along [001] and [010] direction are about $0.576 m_0$ and $1.053 m_0$ (m_0 is free-electron mass), respectively.

References

1. G. Kresse and D. Joubert, *Phys. Rev. B*, 1999, **59**, 1758-1775.
2. G. K. a. J. Hafner, *Phys. Rev. B*, 1993, **47**, 558-561.
3. K. B. John P. Perdew, Matthias Ernzerhof, *Phys. Rev. Let t.*, 1996, **77**, 3865-3868.
4. J. Heyd, G. E. Scuseria and M. Ernzerhof, *J. Chem. Phys.*, 2003, **118**, 8207-8215.
5. J. Heyd, G. E. Scuseria and M. Ernzerhof, *J. Chem. Phys.*, 2006, **124**.